**Structural Engineering and Mechanics**, *Vol. 75, No. 5 (2020) 633-642*
DOI: https://doi.org/10.12989/sem.2020.75.5.633


# Optimization of flexure stiffness of FGM beams via artificial neural networks by mixed FEM

Emrah Madenci*[1] and Şaban Gülcü[2]

*[1]Department of Civil Engineering, Necmettin Erbakan University, 42140 Konya, Turkey*
*[2]Department of Computer Engineering, Necmettin Erbakan University, 42140 Konya, Turkey*

*(Received July 8, 2019, Revised October 1, 2020, Accepted March 15, 2020)*

**Abstract.** Artificial neural networks (ANNs) are known as intelligent methods for modeling the behavior of physical phenomena because of it is a soft computing technique and takes data samples rather than entire data sets to arrive at solutions, which saves both time and money. ANN is successfully used in the civil engineering applications which are suitable examining the complicated relations between variables. Functionally graded materials (FGMs) are advanced composites that successfully used in various engineering design. The FGMs are nonhomogeneous materials and made of two different type of materials. In the present study, the bending analysis of functionally graded material (FGM) beams presents on theoretical based on combination of mixed-finite element method, Gâteaux differential and Timoshenko beam theory. The main idea in this study is to build a model using ANN with four parameters that are: Young's modulus ratio ($E_t/E_b$), a shear correction factor ($k_s$), power-law exponent (n) and length to thickness ratio (L/h). The output data is the maximum displacement (w). In the experiments: 252 different data are used. The proposed ANN model is evaluated by the correlation of the coefficient (R), MAE and MSE statistical methods. The ANN model is very good and the maximum displacement can be predicted in ANN without attempting any experiments.

**Keywords:** functionally graded material beam; artificial neural networks; mixed finite element method; displacement data

## 1. Introduction

The functionally graded materials (FGMs) are advanced composites and play an important role in engineering fields. FGMs have continuously varying fractions of the constituent materials (Madenci 2019). Typically, FGMs are made mixture from metal-ceramic materials thus the ceramic can resist high temperature while the metal can decrease the stresses due to high temperature gradient. Unlike classical layered composites (Kaci *et al*. 2018, Zine *et al*. 2018), FGMs don't have sharp layer changes. In this way, delamination or no sudden stress changes along the thickness coordinate of FGMs. Since FGM structures, and beams in particular, used in several engineering sectors, understanding their behavior is important under load types (Beldjelili *et al*. 2016, Bousahla *et al*. 2016, Gemi *et al*. 2016, Abdelaziz *et al*. 2017, El-Haina *et al*. 2017).

The research reports on flexure stiffness, free vibration, thermal stress and buckling behavior of FGM structures have considerable in the literature during the last decade (Prakash and Ganapathi 2006, Zhang and Zhou 2008, Talha and Singh 2010, Bouderba *et al*. 2013, Belabed *et al*. 2014, Bouhadra *et al*. 2015, Abdelhak *et al*. 2016, Adim and Daouadji 2016, Adim *et al*. 2016, Adim *et al*. 2016, Benferhat *et al*. 2016, Benferhat *et al*. 2016, Daouadji and Adim 2016, Daouadji and Benferhat 2016, El-Haina *et al*. 2017, Nejad *et al*. 2017, Belabed *et al*. 2018, Benyamina *et al*. 2018, Bourada *et al*. 2018, Ebrahimi and Dabbagh 2018, Ersoy *et al*. 2018, Hadi *et al*. 2018, Nejad *et al*. 2018, Solmaz and Civalek 2018, Akgün and Kurtaran 2019, Hadj *et al*. 2019, Rabia *et al*. 2019). But studies on FGM beams are limited (Ziane *et al*. 2015, Trinh1a *et al*. 2016, Mirjavadi *et al*. 2017, Arioui *et al*. 2018). Some of these studies: the thermo-elastic behavior of FGM beams investigated based on first-order shear deformation theory by Chakraborty *et al*. (2003). An elasticity solution for simply-supported FGM beam based on Euler-Bernoulli beam theory was derived by Sankar (2001). Madenci (2019) obtained a refined functional based on general shear deformation beam theories and used for static analysis of FGM beams. The mixed-finite element method is employed to obtain the element matrices. Pradhan and Chakraverty (2013) presented free vibration analysis of FGM beams with the different boundary conditions. The governing equations are obtained by the Rayleigh-Ritz method. Jing *et al*. (2016) developed a finite volume method based on first order shear deformation theory for static and free vibration analysis of FGM beams. The first-order shear deformation beam theory for static and free vibration of axially loaded rectangular functionally graded beams is developed by Nguyen *et al*. (2013).

The design of structures and components using newly advanced composite materials usually requires extensive and expensive testing programs (Gemi 2018, Gemi *et al*. 2018, Gemi *et al*. 2019). Also, the theoretical analysis has more complex equations than isotropic materials (Madenci *et al*. 2020). As mentioned in (Cho and Shin 2004) and (Kou *et al*. 2012), there are some challenges in the design of FGM. Some of them are: a large number of parameters or design variables are required to model heterogeneous FGM

*Corresponding author, Assistant Professor, Ph.D.
E-mail: emadenci@erbakan.edu.tr


http://www.techno-press.com/journals/sem&subpage=7
ISSN: 1225-4568 (Print), 1598-6217 (Online)

distributions, the computational costs and the choice of the sensitivity analysis scheme incorporated with the volume fraction discretization. Therefore the optimum design will provide essential. To tackle the above-mentioned challenges in the design of FGM, an ANN model is proposed in this paper. Artificial neural networks (ANNs) are an effective method for predicting and classifying variables and have emerged as a superior modeling and optimization tool (Peng-hui *et al*. 2015, Yavuz 2016). The ANNs are the information processing method developed by inspiring the human brain's information processing technique. The application areas of ANNs are quite wide which are often used in the field of engineering, science, medicine, business, finance. The ANNs can solve many types of problems. The main ones are the optimization, classification, clustering, and prediction and pattern recognition problems (Hore *et al*. 2016, Karina *et al*. 2017, Zhao *et al*. 2017, Azqandi *et al*. 2018, Chang *et al*. 2019).

ANNs have recently been used in mechanical behavior, monitoring and modeling the manufacturing of composites. Zhang and Friedrich (2003) discussed a review study on the ANNs applied to composite structures. Nielsen and Pitchumani (2001) studied the manufacturing process optimization of composite materials by using ANN. There are many publications on applications of the ANNs for the purpose of prediction for composites (Litak *et al*. 2008, Wang *et al*. 2013). Pidaparti and Palakal (1993) presented modeling of composites using the ANN for predicting the non-linear stress–strain behavior of graphite–epoxy laminates. Labossiere and Turkkan (1993) obtained failure analysis of composites by using polynomial theory and applied ANN to predict under plane stress conditions.

As emphasized in (Kou *et al*. 2012), there are not enough optimization studies for FGM beams. In the aim of this present study, is develop an ANN model that optimization of FGM beams by using soft computing technique. By using variational techniques, mixed finite element matrices of FGM beam is obtained. Then the static analysis is presented and maximum displacements obtained for different effect data combinations. After that, the ANN model is carried out to derive an explicit ANN formulation for the optimization of FGM beam. The model is established within four parameters which are Young's modulus ratio, different shear correction factors, power-law exponent and length to thickness ratio.

Thanks to the ANN technique, we show that optimal FGM design can be flexibly and efficiently conducted.

This article is organized as follows: Section 2 presents the theoretical formulation of FGM beam. The ANN algorithm and the performance metrics are presented in Section 3. Section 4 reveals the experimental results and analysis of ANN in optimization of FGM beams. Finally, the article is concluded in Section 5.

## 2. Theoretical formulation of FGM beam

In this part, the theoretical formulation of FGM beam based on first order shear deformation beam theory via a mixed finite element method is obtained such as Madenci (2019). The partial field equations are transformed to functional and mixed finite element matrices is obtained.

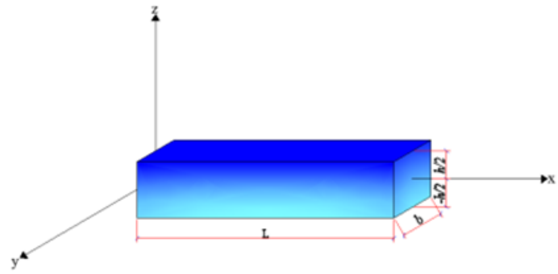


Fig. 1 Geometry of FGM beam

### 2.1 Functionally graded material beam model

In this study FGM beam made of ceramic and metal phases is considered as shown in Figure 1. The cartesian coordinates x-y-z are taken along the length, width, and height of the beam respectively. The geometry of FGM beam, consider a FGM beam with length "L" and rectangular cross section, with "b" being the width and "h" being the height.

The material properties of FGM beams are assumed to vary continuously through the thickness. The power-law distribution method used to calculate the effective material properties which are Young's modulus "$E_{(z)}$", bulk modulus "$G_{(z)}$" and poisson ratio "$\nu_{(z)}$", and given in the general form

$$P_{(z)} = \left(P_t - P_b\right) V_t + P_b \tag{1}$$

where "$P_t$" is the denote the values of the mechanical properties of the top at "$z=h/2$" and bottom at "$z= -h/2$" respectively. In the present study, it is assumed a full metal at the bottom of the FGM beam and a full ceramic at the top of the FGM beam. The parameter "$V_t$" is called volume fraction of FGM beam and defined as

$$V_t = \left(\frac{z}{h} + \frac{1}{2}\right)^n \tag{2}$$

In power-law variation, "$n$" is a power-law exponent and it is a non-negative variable parameter ($n \geq 0$).

### 2.2 Kinematics

The purposed mathematical model can be represented in terms of first order shear deformation beam theory as

$$U(x,z) = z\phi_x; \quad V(x,z) = 0; \quad W(x,z) = w_0 \tag{3}$$

where "$w_0$" is the transverse displacement, "$\phi_x$" is the total bending rotation of the cross-section at any point on the neutral axis.

The non-zero strains are given by

$$\varepsilon_x = \frac{\partial U}{\partial x} = z\frac{\partial \phi_x}{\partial x}, \quad \gamma_{xz} = \frac{\partial U}{\partial z} + \frac{\partial W}{\partial x} = \phi_x + \frac{\partial w_x}{\partial x} \tag{4}$$

For the FGM beam, the external and internal virtual work expressions can be written as

$$\int_{\Omega_0} \mathbf{F}\cdot\delta\mathbf{u}\,dV - \int_{\Omega_0} \mathbf{f}\cdot\delta\mathbf{u}\,dV = 0 \tag{5}$$

where the first integral " $\int_{\Omega_0} \mathbf{F}\cdot\delta\mathbf{u}\,dV$ " is total internal works and the second integral " $\int_{\Omega_0} \mathbf{f}\cdot\delta\mathbf{u}\,dV$ " is total external works done, respectively. The virtual work done by actual forces "**F**" and body forces "**f**" in a body "$\Omega_0$" in moving through the virtual displacements " $\delta\mathbf{u}$ " is given by

$$\delta\mathbf{u} = \begin{bmatrix} \delta\varepsilon_x \\ \delta\gamma_{xz} \\ \delta w \end{bmatrix}, \qquad \mathbf{F} = \begin{bmatrix} \sigma_x \\ \tau_{xz} \end{bmatrix}, \qquad \mathbf{f} = \left[q(x)\right] \tag{6}$$

Variation of virtual work calculated by

$$\int_0^L \int_A [\sigma_x\,\delta\varepsilon_x + \tau_{xz}\,\delta\gamma_{xz}]\,dAdx - \int_0^L q_{(x)}\,\delta w\,dx = 0 \tag{7}$$

Substituting Eq. (4) into Eq. (7) and integrating through the thickness of FGM beam, it can be rewritten in (Özütok and Madenci 2013)

$$\left.\begin{aligned} &\int_0^L \int_A \left[\sigma_x\, z\delta\phi_{x,x} + \tau_{xz}\,\delta\phi_x + \tau_{xz}\,\delta w_{,x}\right] dAdx \\ &-\int_0^L q_{(x)}\,\delta w\,dx = 0 \\ &\int_0^L \left\{M_x\,\delta\phi_{x,x} + Q_x\,\delta\phi_x + Q_x\,\delta w_{,x}\right\} dx \\ &-\int_0^L q_{(x)}\,\delta w\,dx = 0 \end{aligned}\right\} \tag{8}$$

Stress resultants bending moment "$M_x$" and shear force "$Q_x$" are defined by

$$\left\{M_x, Q_x\right\} = \int_A \left\{\sigma_x, \tau_{xz}\right\} \begin{Bmatrix} z \\ 1 \end{Bmatrix} dz \tag{9}$$

The Eular-Lagrange equations can be derived from Eq. (8) by integration the displacement gradients by parts and setting the coefficient " $\delta w$ " and " $\delta\phi_x$ " to zero separately. Then, the Euler-Lagrange equations can be obtained as

$$\left.\begin{aligned} \partial w : 0 \rightarrow \quad -Q_{x,x} - q = 0 \\ \partial\phi_x : 0 \rightarrow \quad -M_{x,x} + Q_x = 0 \end{aligned}\right\} \tag{10}$$

Using the material properties in Eq. (1), the linear constitutive relations are

$$\begin{Bmatrix} \sigma_x \\ \tau_{xz} \end{Bmatrix} = \begin{bmatrix} Q_{11} & 0 \\ 0 & Q_{55} \end{bmatrix} \begin{Bmatrix} \varepsilon_x \\ \gamma_{xz} \end{Bmatrix} \tag{11}$$

where " $\sigma_x, \tau_{xz}$ " and " $\varepsilon_x, \gamma_{xz}$ " are terms of the stresses and deformations, respectively. The transformed stiffness constants in the beam coordinate system are defined as

$$Q_{11} = \frac{E_{(z)}}{1-(v_z)^2}, \quad Q_{55} = G_{(z)} = \frac{E_{(z)}}{2(1+v_z)} \tag{12}$$

Substituting Eqs. (10,11) into Eq. (9) and integrating through the thickness of The FGM beam, following constitutive equations are obtained

$$\begin{bmatrix} M_x \\ Q_x \end{bmatrix} = \begin{bmatrix} D_{11} & 0 \\ 0 & A_{55} \end{bmatrix} \begin{Bmatrix} \varepsilon_x \\ \gamma_{xz} \end{Bmatrix} \tag{13}$$

Extensional stiffness " $A_{55}$ " and bending stiffness " $D_{11}$ " are defined as follows

$$\left\{D_{11},\, A_{55}\right\} = \int_{-h/2}^{h/2} (E_{(z)}, G_{(z)}) \begin{Bmatrix} z^2 \\ k_s \end{Bmatrix} dz \tag{14}$$

The " $k_s$ " denote the shear correction factor for first order shear deformation theory that doesn't neglect the effect of the transverse shear deformation and consider a uniform transverse shear stress distribution through the beam thickness. Therefore, needs a shear correction factor to assume a linear shear deformation across the thickness of the beam.

### *2.3 Variational formulations and mixed finite element matrix*

Eq. (10) and Eq. (13) obtained by combining the partial differential equilibrium and constitutive equations of the field equations are written in the operator form and after showing the potential of the first order shear deformation theory obtained by applying the variational methods of FGM beams depending on the function is derived. The procedure is summarized in (Eratll and Aköz 1997, Kadioglu and Akoz 2003, Özütok and Madenci (2017), Madenci 2019). The functional for the FGM beam based on first order shear deformation theory for the chosen mixed formulation written in terms of independent variables and dynamic and geometric boundary conditions as follows

$$\begin{aligned} \mathbf{I}(\mathbf{y}) = {} & [Q_x, \frac{\partial w}{\partial x}] + [M_x, \frac{\partial\phi_x}{\partial x}] + [Q_x, \phi_x] - \frac{1}{2D_{11}}[M_x, M_x] \\ & - \frac{1}{2A_{55}}[Q_x, Q_x] - \left[q, w\right] - [\hat{\mathbf{M}}, \mathbf{\Omega}]_\varepsilon - [\hat{\mathbf{R}}, \mathbf{w}]_\varepsilon \\ & - [\mathbf{R}, (\mathbf{w} - \hat{\mathbf{w}})]_\sigma - [(\mathbf{\Omega} - \hat{\mathbf{\Omega}}), \mathbf{M}]_\sigma \end{aligned} \tag{15}$$

Then, taking variations and equating to zero, allows obtaining eight linearly independent equations since the variable variations are arbitrary and independent. The independent variables are expressed in terms of interpolation functions as "w, $\phi_x$, $M_x$, $Q_x$, $\frac{\partial w}{\partial x}, \frac{\partial\phi_x}{\partial x}$".

$$[k_{el}] = \left[\begin{array}{cccc:cccc} 0 & 0 & 0 & -\frac{1}{2} & 0 & 0 & 0 & -\frac{1}{2} \\ 0 & 0 & -\frac{1}{2} & \frac{L}{3} & 0 & 0 & -\frac{1}{2} & \frac{L}{6} \\ 0 & \frac{1}{2} & -\frac{L}{3D_{11}} & 0 & 0 & \frac{1}{2} & -\frac{L}{6D_{11}} & 0 \\ \frac{1}{2} & 0 & 0 & -\frac{L}{3A_{11}} & \frac{1}{2} & 0 & 0 & -\frac{L}{6A_{11}} \\ \hdashline 0 & 0 & 0 & \frac{1}{2} & 0 & 0 & 0 & \frac{1}{2} \\ 0 & 0 & \frac{1}{2} & \frac{L}{6} & 0 & 0 & \frac{1}{2} & \frac{L}{3} \\ 0 & -\frac{1}{2} & -\frac{L}{6D_{11}} & 0 & 0 & -\frac{1}{2} & -\frac{L}{3D_{11}} & 0 \\ -\frac{1}{2} & 0 & 0 & -\frac{L}{6A_{11}} & -\frac{1}{2} & 0 & 0 & -\frac{L}{3A_{11}} \end{array}\right] \left\{\begin{array}{c} w_1 \\ \phi_{x1} \\ M_{x1} \\ Q_{x1} \\ \hdashline w_2 \\ \phi_{x2} \\ M_{x2} \\ Q_{x2} \end{array}\right\} \quad (16)$$

The approach utilized here to obtain the mixed finite element method is explained in detail in (Özütok and Madenci (2013), Ozutok *et al*. 2014, Madenci and Özütok 2020) for the case of laminated composite beams. The functional is extremized with respect to nodal variables then the mixed finite element matrices is obtained in Eq. (16). Thus, the mixed finite element matrices of FGM beam element based on first order order shear deformation theory which has four degree-of-freedom at the per node, total eight, is obtained for static deformation analysis. The unknowns are displacement, rotation, moment and shear force in Eq. (16).

## 3. Artificial neural networks (ANNs)

ANNs simulate the operation of the simple biological nervous system. The cells of the biological nervous system are called neurons (Rastbood *et al*. 2017). Neurons are connected to each other in various ways to form a network. Thus, neurons in ANNs can gain the ability of the biological nervous system. These networks are capable of learning, memorizing and revealing the relationship between data (Aggarwal 2018).

There are various types of ANNs and it can be classified according to the number of layers, the topology and learning algorithm (Bahadır and Balık 2017). Some types are the feed forward, recurrent, single-layer, multi-layer, supervised and unsupervised networks. The main feature of the ANNs is the learning ability. This learning ability is realized by updating the weights of ANNs using the learning algorithms. In this paper, the feed forward back propagation neural network is used to solve the prediction problem. An ANN is composed of layers such as input layer, hidden layers, and output layer. The number of the hidden layers are defined by the user. The main structure of the ANN is shown in Fig. 2. Each layer has at least one neuron. Data are given to the input layer. The ANN processes the data and the output layer presents the result to the user.

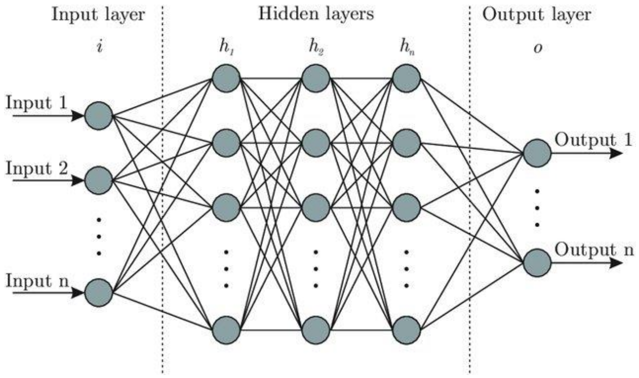


Fig. 2 The main structure of the artificial neural network (Bre *et al*. 2018)

In the ANNs, the neurons work principle as follows: Each neuron has at least one input and only one output. These inputs are connected to the neuron through weights. also the input of another neuron. To process the data, the inputs of the neuron are multiplied with its weights. Thus, the effect of the input is scaled. After that, the calculated The output of a neuron except the neurons in the output layer is value is given to a function, called the activation function. Equation (17) shows how the neuron $j$ processes the data to generate an output.

$$y_j = f(b_j + \sum\nolimits_{i=1}^{m} w_{ij} x_i) \quad (17)$$

Here $y_j$ is the output of the neuron $j$, $x_i$ is the input, $b_j$ is the bias, $w_{ij}$ is the weight and $f(.)$ is the activation function. One of the most important factors determining neuron behavior is the activation function. The result of the product of the inputs and weights is converted to the output of the neuron by the activation function. Thanks to the activation function, the ANN generates a linear or nonlinear model. The most used activation functions are the sigmoid, hyperbolic tangent, rectified linear unit, and softmax function. In this paper, the sigmoid activation function is used and its formulation is given in Eq. (18).

$$f(a) = 1/(1 + e^{-a}) \quad (18)$$

The steps of the application of the artificial neural network are as follows:

- collecting data
- preparing data
- defining network architecture
- initializing weights and bias
- training network
- validating network
- using network

### *3.1 Collecting data*

The collecting data is the first step of the application of the ANN learns from the data. Therefore, data should coherent and should not contain missing values. To create a good neural network, 252 different design mixed data-set obtained based on static analysis of simply-supported FGM beam by using Eq. (16). Where the input data are non-dimensional Young's modulus ratio ($E_t/E_b$), a shear correction factor ($k_s$) as Jing *et al*. (2016), power-law exponent ($n$) and length to thickness ratio ($L/h$); output data is maximum displacement ($w$) respectively. The combination parameters of input data are given in Table 1.

Table 1 Input data values

| Et/Eb | ks | n | L/h |
|---|---|---|---|
| 0.25 | 1 | 0 | 4 |
| 0.50 | 2 | 0.2 | 16 |
| 1 | 3 | 0.5 | |
| 2 | | 1 | |
| 4 | | 2 | |
| 6 | | 5 | |
| | | 10 | |

Table 2 Statistical analysis of data

| Attribute | Min | Max | Mean | St. Dev. |
|---|---|---|---|---|
| Et/Eb | 0.25 | 6.00 | 2.29 | 2.08 |
| ks | 1.00 | 3.00 | 2.00 | 0.82 |
| n | 0.00 | 10.00 | 2.67 | 3.39 |
| L/h | 4.00 | 16.00 | 10.00 | 6.01 |
| w | 0.17 | 4.63 | 1.03 | 0.77 |

Using the statistical parameters of the data are shown in Table 2.

### *3.2 Preparing data*

The preparing data is the second step of the application of the ANN. In this step, the data are randomly divided into three distinct subsets (train, validation, and test). The ANN is trained using the train data. The prevention of overtraining on the training data is a key function performed by the validation data set. After that, the performance quality of the model of the ANN is evaluated using the test data (Cain 2016). And then, the ANN is ready to use. In this paper, the train data are 70% of the data, the validation data are 15% of the data, and the test data are 15% of the data.

### *3.3 Defining network architecture*

As shown in Fig. 2, an ANN is composed of an input layer consists of input neurons which take the data from the outside, an output layer consists of output neurons which give the result of the ANN to the outside and one or more hidden layers between the input layer and the output layer. The architecture of an ANN affects the success of the prediction. Therefore, defining network architecture is an important step. The following variables must be determined in the design of the ANN: the number of input neurons, the number of hidden layers and hidden neurons, number of output neurons. The selection of these parameters varies according to the problem.

The number of independent variables of the problem gives the number of input neurons of the ANN. The number of dependent variables of the problem gives the number of output neurons of the ANN. The important factor in the optimization of the ANN is to determine the number of the hidden layers and the number of neurons in these layers. The ANN with one hidden layer is successful in solving problems. However, sometimes 2 hidden layers may be needed when working with data that contain a very complex structure. Increasing the number of hidden layers causes the increase of the calculation time. In this study, there are 4 neurons in the input layer since the number of the independent variables is 4 and there is 1 neuron in the output layer since the number of the dependent variable is 1. There is no fixed rule in determining the number of neurons in the hidden layer. It is usually started with a small number of neurons and is increased to a certain limit. In this study, the number of hidden neurons was started at 2 and was tried in order up to 10. Therefore, 9 different architectures were used to find the best model. In the ANN, activation functions affect the success of the prediction. In this study, the sigmoid activation function was used and its formulation is given in Eq. (2).

### *3.4 Initializing weights and bias*

The initial values of the weights and biases affect finding the global optimum by the ANN. The initial values should be neither too big nor too small. A general approach is to assign the initial values in the range [-0.5, 0.5] or [-1, 1] (Raschka 2015, Rashid (2016)). In this study, the initial values of the weights and biases were generated randomly in the range [-1, 1].

### *3.5 Training network*

The ANNs are a learning system with the help of examples. An objective function must be defined to measure the training performance of the network that is established and trained according to the problem. The mean square error in Eq. (5) is usually used as the objective function of ANNs, because it is defined in relation to the error term. In this study, the mean square error was used as the objective function of the artificial neural network, too. Furthermore, 70% of the data were used as the train data. In ANNs, there are many algorithms to train the network. One of the most popular and most widely used algorithms is the back-propagation algorithm (Skorpil and Stastny 2006). In this study, the back-propagation algorithm was used. A stop criterion should be determined before the back-propagation algorithm trains the network. This stop criterion is usually the maximum number of iterations. Training of the ANN by the backpropagation algorithm consists of 3 steps: The network input moves from the input layer to the output layer. Calculation of the error in the output layer and backward propagation. Updating the weights according to the error propagated backward. These steps continue until the maximum iteration number is reached. When the maximum iteration number is reached, training of the ANN is completed. In this way, ANNs with different network architectures are trained in order.

### *3.6 Validating network*

After the training is completed, the operation of the artificial neural network is always forward. The trained network receives the input from the outside using the input neurons and gives the result to the outside using the output neurons. Although the training of the artificial neural network takes a long time, generating the result of the network for the new input data is very fast. To determine and compare the success rates of the ANNs with the different network architectures, these are tested with a validation dataset. Thus, the best performing ANN among them is put into use. In this study, 15% of the data were used as the validation dataset.

### *3.7 Using network*

The trained network receives the input from the outside using the input neurons and gives the result to the outside using the output neurons. Although the training of the ANN takes a long time, the test of the trained network using the test data is very fast. After determining the best performance ANN using the validation dataset, it is ready to use and its performance is measured using the test data. This test data is a dataset that the network has never used before. In this study, the test data are 15% of the data.

### *3.8 Performance metrics*

The performance of an ANN can be evaluated in terms of computational time and estimation accuracy (Twomey and Smith 1995). The estimation accuracy is determined by the analysis of estimation errors. The estimation error is the difference between the actual observation value and the estimated value. In this study, in order to measure the accuracy of estimation, the statistical metrics which are frequently used in literature were used. These metrics are the correlation of the coefficient (R), the mean square error (MSE) and the mean absolute error (MAE). Their formulations are given in Eqs. (19)-(21).

$$R = \sqrt{1 - \left(\sum_{i=1}^{N} (O_i - P_i)^2 \Big/ \sum_{i=1}^{N} (O_i - \bar{P})^2\right)} \tag{19}$$

$$MAE = \left(\sum_{i=1}^{N} |O_i - P_i|\right) \Big/ N \tag{20}$$

$$MSE = \left(\sum_{i=1}^{N} (O_i - P_i)^2\right) \Big/ N \tag{21}$$

Here $N$ is the number of the instances, $O$ is the observed value, $P$ is the predicted value, and $\bar{P}$ is the mean of the predicted values.

## 4. Experimental Results

In this section, the experimental results are presented. The technical features of the computer used in the experiments are as follows: Windows 10 operating system, intel i5 3 GHz, 4 GB memory, visual studio 2017, C# programming language. In this study, the number of hidden neurons was started at 2 and was tried in order up to 10. Therefore, 9 different architectures were used to find the best model. According to the experimental results, the hidden layer in the best model has 10 neurons. The architecture of the best model is 4-10-1. The values of the parameters used in the study are as follows: the number of the layers is 3 (input, hidden and output). The number of neurons in the input layer is 4, the number of neurons in the hidden layer is 10, and the number of neurons in the output layer is 1. The momentum and learning rate is 0.8 and 0.3, respectively. The maximum epoch number is 1000.

The formulation of the generated model is shown in Eq. (22). The function *f*(.) represents the sigmoid activation function whois formulation is given in Eq. (18).

$$Y = f(\,f(X * IHW + b_1) * HOW + b_2) \tag{22}$$

Where $X$ represents the input values. $b_1$ represents the biases of the neurons in the hidden layer and $b_2$ represents the biases of the neurons in the output layer. $IHW$ represents the weights between the input layer and the hidden layer and $HOW$ represents the weights between the hidden layer and the output layer. The values of the $b_1$, $b_2$, $IHW$, and $HOW$ of the best model are given in Table 3 and Table 4.

Table 5 shows the performance of the proposed ANN model. The values of the correlation of the coefficient (R) for the training, validation and test are 0.98, 0.982 and 0.962, respectively. The larger the coefficient, the stronger the relationship, so that a correlation that is close to one indicates a very strong relationship, while coefficients that are near zero indicate very weak relationships (Bachman 2004). Because the values of the correlation of the coefficient (R) for the training, validation and test are close to one, there is a very strong relationship. The values of the mean absolute error (MAE) for the training, validation and test are 0.051, 0.056 and 0.08, respectively. The values of the mean square error (MSE) for the training, validation, and test are 0.012, 0.007 and 0.027, respectively. Lower MSE and lower MAE indicate more accurate prediction.

Fig. 3 shows the regression plots of the proposed ANN model. According to the plots for the training, validation, and test, the prediction performance of the proposed ANN model is very good.

Table 3 The weights of the hidden layer

| IHW | | | |
|---|---|---|---|
| 1,0427 | -0,1787 | -0,4650 | 0,0630 |
| -19,6590 | -0,1219 | -28,4935 | -0,3401 |
| 1,8004 | -0,2771 | -1,2107 | 0,7198 |
| -0,0469 | -1,3333 | 0,1599 | -1,1096 |
| -0,7450 | -0,4551 | 0,3612 | -0,5389 |
| 1,6648 | -0,0347 | -8,2349 | -0,5327 |
| 5,2911 | -0,1071 | 1,6932 | 0,0603 |
| -0,1657 | 0,1117 | -0,4491 | -0,4757 |
| 0,2515 | 0,0055 | 0,1567 | -1,2077 |
| 2,3480 | 0,8533 | 0,2010 | 0,0572 |

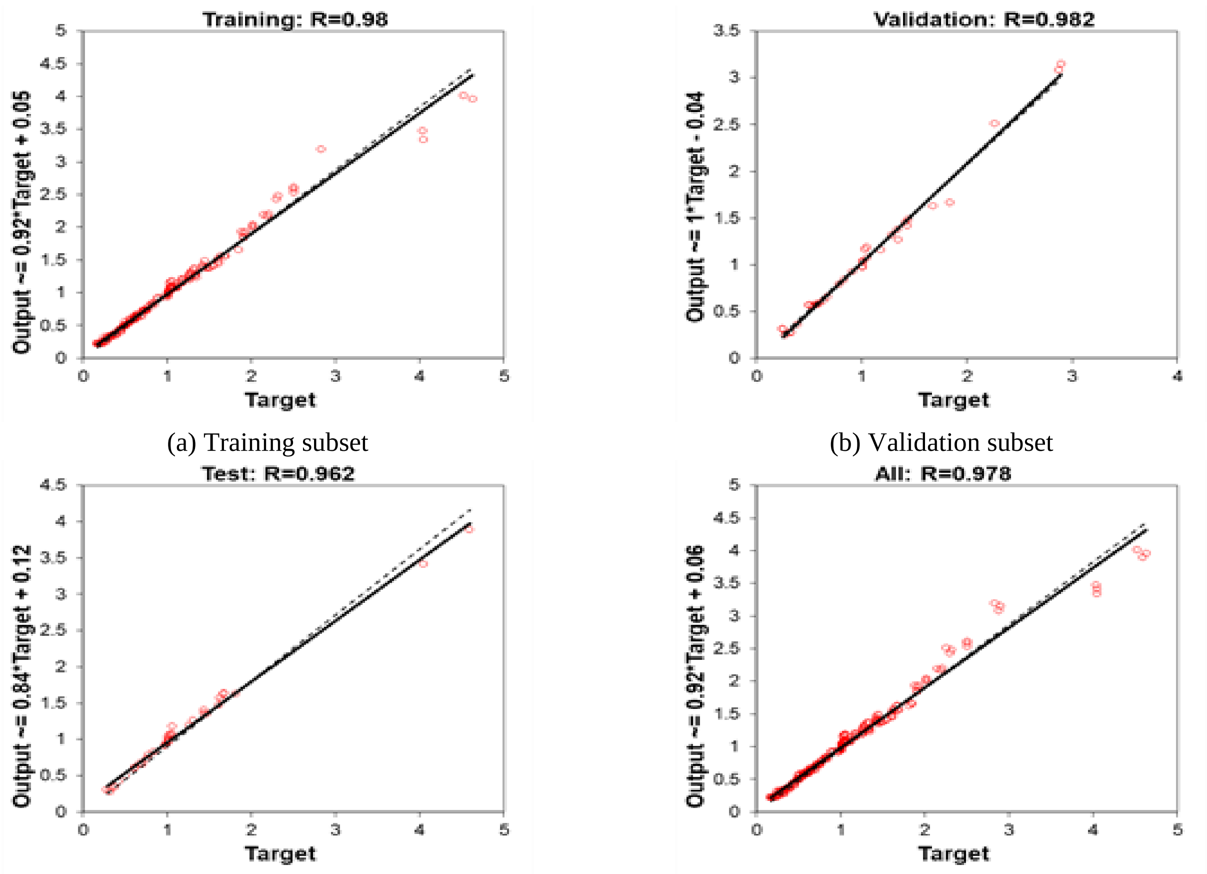


(a) Training subset (b) Validation subset

(c) Test subset (d) All data

Fig. 3 The regression results of the training, validation, test and all data

Table 4 The weights of the biases and the output layer

| b1 | HOW | b2 |
|---|---|---|
| -1,8382 | -0,7078 | 0,4827 |
| -1,4196 | 15,4210 | |
| -1,6723 | -1,5432 | |
| -1,5416 | -0,4508 | |
| -1,5761 | 0,5240 | |
| -1,7193 | -3,5549 | |
| -0,3296 | -1,8421 | |
| -2,0542 | 0,1376 | |
| -1,7314 | 0,3614 | |
| -2,0223 | -0,6749 | |

Table 5 Performance of the proposed ANN model

| Criteria | Training | Validation | Test |
|---|---|---|---|
| Instance | 176 | 38 | 38 |
| R | 0.980 | 0.982 | 0.962 |
| MAE | 0.051 | 0.056 | 0.080 |
| MSE | 0.012 | 0.007 | 0.027 |

Fig. 4 shows the error histogram plot of the proposed ANN model. It provides additional verification of the performance of the artificial neural network. It indicates outliers. The blue, green and red areas represent training, validation and test data respectively.

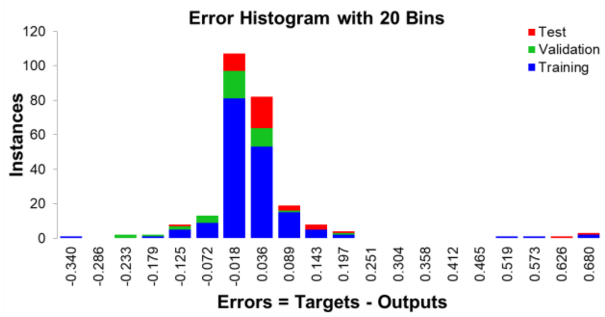


Fig. 4 The error histogram

The most data fall on zero error which provides an idea to check the outliers to determine if the data is bad, or if those data points are different than the rest of the data set. If the outliers are valid data points, but are unlike the rest of the data, then the network is extrapolating for these points (Yadav *et al*. 2015). As shown in Fig. 4, the density in the diagram is around zero. Therefore, the prediction success of the network is very high.

## 5. Conclusions

The proposed ANN based model was performed well for maximum displacement of FGM beams such as Young modulus ratio, length to thickness ratio, effect of shear correction factor, effect of power-low exponent. The main feature of the ANN is the learning ability. It learns from data. The main aim of this study is to develop a model which may predict the maximum displacement. The proposed ANN model is composed of one input layer, one output layer and one hidden layer between the input layer and the output layer. The architecture of the model is 4-10-1.

In the experiments, we used 252 different data. The input data are the non-dimensional Young's modulus ratio ($E_t/E_b$), a shear correction factor ($k_s$), power-law exponent ($n$) and length to thickness ratio ($L/h$). The output data is the maximum displacement ($w$). The train data are 70% of the data, the validation data are 15% of the data, and the test data are 15% of the data. The proposed ANN model is evaluated by the correlation of the coefficient (R), MAE and MSE statistical methods. The values of the R for the training, validation and test are 0.98, 0.982 and 0.962, respectively. Additionally, the values of the MAE and MSE are close to zero. In conclusion, the prediction ability of the ANN model is very good and the maximum displacement can be predicted in ANN without attempting any experiments. Thanks to the ANN technique, we show that optimal FGM design can be flexibly and efficiently conducted.

## Acknowledgments

The research described in this paper was financially supported by the Necmettin Erbakan University, Natural Scientific Research Project (BAP) Project No: 181219012

## References

Abdelaziz, H. H., M. A. A. Meziane, A. A. Bousahla, A. Tounsi, S. Mahmoud and A. S. Alwabli (2017), "An efficient hyperbolic shear deformation theory for bending, buckling and free vibration of FGM sandwich plates with various boundary conditions", *Steel Compos. Struct.,* **25**(6), 693-704. https://doi.org/10.12989/scs.2017.25.6.693.

Abdelhak, Z., L. Hadji, T. H. Daouadji and E. Adda Bedia (2016), "Thermal buckling response of functionally graded sandwich plates with clamped boundary conditions", *Smart Struct. Syst.,* **18**(2), 267-291. https://doi.org/10.12989/sss.2016.18.2.267.

Adim, B. and T. H. Daouadji (2016), "Effects of thickness stretching in FGM plates using a quasi-3D higher order shear deformation theory", *Adv. Mater. Res.,* **5**(4), 223. http://dx.doi.org/10.12989/amr.2016.5.4.223.

Adim, B., T. H. Daouadji and B. Abbes (2016), "Buckling analysis of anti-symmetric cross-ply laminated composite plates under different boundary conditions", *Appl. Mech.,* **52**(6), 661-676. https://doi.org/10.1007/s10778-016-0787-x.

Adim, B., T. H. Daouadji, B. Rabia and L. Hadji (2016), "An efficient and simple higher order shear deformation theory for bending analysis of composite plates under various boundary conditions", *Earthq. Struct.,* **11**(1), 63-82. https://doi.org/10.12989/eas.2016.11.1.063.

Aggarwal, C.C. (2018), *Neural Networks and Deep Learning*, Springer, Germany.

Akgün, G. and H. Kurtaran (2019), "Large displacement transient analysis of FGM super-elliptic shells using GDQ method", *Thin. Wall. Struct.* **141**: 133-152. https://doi.org/10.1016/j.tws.2019.03.049.

Arioui, O., K. Belakhdar, A. Kaci and A. Tounsi (2018), "Thermal buckling of FGM beams having parabolic thickness variation and temperature dependent materials", *Steel Compos. Struct.,* **27**(6), 777-788. https://doi.org/10.12989/scs.2018.27.6.777.

Azqandi, M. S., N. Nooredin and A. Ghoddosian (2018), "Optimization of spring back in U-die bending process of sheet metal using ANN and ICA", *Struct. Eng. Mech.,* **65**(4), 447-452. https://doi.org/10.12989/sem.2018.65.4.447.

Bachman, L.F. (2004), *Statistical Analyses for Language Assessment Book*, Cambridge University Press, United Kingdom.

Bahadır, F. and F. S. Balık (2017), "Predicting Displacement Data of Three-Dimensional Reinforced Concrete Frames with Different Strengthening Applications Using ANN", *Periodica Polytechnica Civil Eng.,* **61**(4), 843-856. https://doi.org/10.3311/PPci.9652.

Belabed, Z., A. A. Bousahla, M. S. A. Houari, A. Tounsi and S. Mahmoud (2018), "A new 3-unknown hyperbolic shear deformation theory for vibration of functionally graded sandwich plate", *Earthq. Struct.,* **14**(2), 103-115. https://doi.org/10.12989/eas.2018.14.2.103.

Belabed, Z., M. S. A. Houari, A. Tounsi, S. Mahmoud and O. A. Bég (2014), "An efficient and simple higher order shear and normal deformation theory for functionally graded material (FGM) plates", *Compos. Part B. Eng.,* **60**: 274-283. https://doi.org/10.1016/j.compositesb.2013.12.057.

Beldjelili, Y., A. Tounsi and S. Mahmoud (2016), "Hygro-thermo-mechanical bending of S-FGM plates resting on variable elastic foundations using a four-variable trigonometric plate theory", *Smart Struct. Syst.,* **18**(4), 755-786. https://doi.org/10.12989/sss.2016.18.4.755.

Benferhat, R., T. H. Daouadji and B. Adim (2016), "A novel higher order shear deformation theory based on the neutral surface concept of FGM plate under transverse load", *Adv. Mater. Res.,* **5**(2), 107. http://dx.doi.org/10.12989/amr.2016.5.2.107.

Benferhat, R., T. Hassaine Daouadji, L. Hadji and M. Said Mansour (2016), "Static analysis of the FGM plate with porosities", *Steel Compos. Struct.,* **21**(1), 123-136. https://doi.org/10.12989/scs.2016.21.1.123.

Benyamina, A. B., B. Bouderba and A. Saoula (2018), "Bending Response of Composite Material Plates with Specific Properties, Case of a Typical FGM" Ceramic/Metal" in Thermal Environments", *Periodica Polytech. Civil Eng.,* **62**(4), 930-938. https://doi.org/10.3311/PPci.11891.

Bouderba, B., M. S. A. Houari and A. Tounsi (2013), "Thermomechanical bending response of FGM thick plates resting on Winkler-Pasternak elastic foundations", *Steel Compos. Struct.,* **14**(1), 85-104. https://doi.org/10.12989/scs.2013.14.1.085.

Bouhadra, A., S. Benyoucef, A. Tounsi, F. Bernard, R. B. Bouiadjra and M. Sid Ahmed Houari (2015), "Thermal buckling response of functionally graded plates with clamped boundary conditions", *J. Therhaml. Stress.,* **38**(6), 630-650. https://doi.org/10.1080/01495739.2015.1015900.

Bourada, F., K. Amara, A. A. Bousahla, A. Tounsi and S. Mahmoud (2018), "A novel refined plate theory for stability analysis of hybrid and symmetric S-FGM plates", *Struct. Eng. Mech.,* **68**(6), 661-675. https://doi.org/10.12989/sem.2018.68.6.661.

Bousahla, A. A., S. Benyoucef, A. Tounsi and S. Mahmoud (2016), "On thermal stability of plates with functionally graded coefficient of thermal expansion", *Struct. Eng. Mech.,* **60**(2), 313-335. https://doi.org/10.12989/sem.2016.60.2.313.

Bre, F., J. M. Gimenez and V. D. Fachinotti (2018), "Prediction of wind pressure coefficients on building surfaces using artificial neural networks", *Energy and Build.*, **158**, 1429-1441. https://doi.org/10.1016/j.enbuild.2017.11.045.

Cain, G. (2016), *Artificial Neural Networks: New Research*, Nova Science Publishers, New York, USA.

Chakraborty, A., S. Gopalakrishnan and J. Reddy (2003), "A new beam finite element for the analysis of functionally graded materials", *J. Mech. Sci.,***45**(3), 519-539. https://doi.org/10.1016/S0020-7403(03)00058-4.

Chang, M., J. K. Kim and J. Lee (2019), "Hierarchical neural network for damage detection using modal parameters", *Struct. Eng. Mech.,* **70**(4), 457-466. https://doi.org/10.12989/sem.2019.70.4.457.

Cho, J. and S. Shin (2004), "Material composition optimization for heat-resisting FGMs by artificial neural network", *Compos. Part A Appl. Sci. Manufact.,* **35**(5), 585-594. https://doi.org/10.1016/j.compositesa.2003.12.003.

Daouadji, T. H. and B. Adim (2016), "An analytical approach for buckling of functionally graded plates", *Adv. Mater. Res.,* **5**(3), 141. http://dx.doi.org/10.12989/amr.2016.5.3.141.

Daouadji, T. H. and R. Benferhat (2016), "Bending analysis of an imperfect FGM plates under hygro-thermo-mechanical loading with analytical validation", *Adv. Mater. Res.,* **5**(1), 035. http://dx.doi.org/10.12989/amr.2016.5.1.035.

Ebrahimi, F. and A. Dabbagh (2018), "NSGT-based acoustical wave dispersion characteristics of thermo-magnetically actuated double-nanobeam systems", *Struct. Eng. Mech.,* **68**(6), 701-711. https://doi.org/10.12989/sem.2018.68.6.701.

El-Haina, F., A. Bakora, A. A. Bousahla, A. Tounsi and S. Mahmoud (2017), "A simple analytical approach for thermal buckling of thick functionally graded sandwich plates", *Struct. Eng. Mech.,* **63**(5), 585-595. https://doi.org/10.12989/sem.2017.63.5.585.

Eratll, N. and A. Aköz (1997), "The mixed finite element formulation for the thick plates on elastic foundations", *Comput. Struct.,* **65**(4), 515-529. https://doi.org/10.1016/S0045-7949(96)00403-8.

Ersoy, H., K. Mercan and Ö. Civalek (2018), "Frequencies of FGM shells and annular plates by the methods of discrete singular convolution and differential quadrature methods", *Compos. Struct.,***183**, 7-20. https://doi.org/10.1016/j.compstruct.2016.11.051.

Gemi, L. (2018), "Investigation of the effect of stacking sequence on low velocity impact response and damage formation in hybrid composite pipes under internal pressure. A comparative study", *Compos. Part B. Eng.,* **153**: 217-232. https://doi.org/10.1016/j.compositesb.2018.07.056.

Gemi, L., C. Aksoylu, Ş. Yazman, Y. O. Özkılıç and M. H. Arslan (2019), "Experimental investigation of shear capacity and damage analysis of thinned end prefabricated concrete purlins strengthened by CFRP composite", *Compos. Struct.*, 111399. https://doi.org/10.1016/j.compstruct.2019.111399.

Gemi, L., M. Kara and A. Avci (2016), "Low velocity impact response of prestressed functionally graded hybrid pipes", *Compos. Part B. Eng.,* **106**, 154-163. https://doi.org/10.1016/j.compositesb.2016.09.025.

Gemi, L., M. Kayrıcı, M. Uludağ, D. S. Gemi and Ö. S. Şahin (2018), "Experimental and statistical analysis of low velocity impact response of filament wound composite pipes", *Compos. Part B. Eng.,* **149**, 38-48. https://doi.org/10.1016/j.compositesb.2018.05.006.

Hadi, A., M. Z. Nejad, A. Rastgoo and M. Hosseini (2018), "Buckling analysis of FGM Euler-Bernoulli nano-beams with 3D-varying properties based on consistent couple-stress theory", *Steel Compos. Struct.,* **26**(6), 663-672. https://doi.org/10.12989/scs.2018.26.6.663.

Hadj, B., B. Rabia and T. H. Daouadji (2019), "Influence of the distribution shape of porosity on the bending FGM new plate model resting on elastic foundations", *Struct. Eng. Mech.,* **72**(1), 61-70. https://doi.org/10.12989/sem.2019.72.1.061.

Hore, S., S. Chatterjee, S. Sarkar, N. Dey, A. S. Ashour, D. Balas-Timar and V. E. Balas (2016), "Neural-based prediction of structural failure of multistoried RC buildings", *Struct. Eng. Mech.,* **58**(3), 459-473. http://dx.doi.org/10.12989/sem.2016.58.3.459.

Jing, L.-l., P.-j. Ming, W.-p. Zhang, L.-r. Fu and Y.-p. Cao (2016), "Static and free vibration analysis of functionally graded beams by combination Timoshenko theory and finite volume method", *Compos. Struct.,***138**, 192-213. https://doi.org/10.1016/j.compstruct.2015.11.027.

Kaci, A., M. S. A. Houari, A. A. Bousahla, A. Tounsi and S. Mahmoud (2018), "Post-buckling analysis of shear-deformable composite beams using a novel simple two-unknown beam theory", *Struct. Eng. Mech.,* **65**(5), 621-631. https://doi.org/10.12989/sem.2018.65.5.621.

Kadioglu, F. and A. Y. Akoz (2003), "The mixed finite element for quasi-static and dynamic analysis of viscoelastic circular beams", *Struct. Eng. Mech.,* **15**(6), 735-752. https://doi.org/10.12989/sem.2003.15.6.735.

Karina, C. N., P.-j. Chun and K. Okubo (2017), "Tensile strength prediction of corroded steel plates by using machine learning approach", *Steel Compos. Struct.,* **24**(5), 635-641. https://doi.org/10.12989/scs.2017.24.5.635.

Kou, X., G. T. Parks and S. T. Tan (2012), "Optimal design of functionally graded materials using a procedural model and particle swarm optimization", *Comput.-Aided Design,* **44**(4), 300-310. https://doi.org/10.1016/j.cad.2011.10.007.

Labossiere, P. and N. Turkkan (1993), "Failure prediction of fibre-reinforced materials with neural networks", *J. Reinforced Plastics Compos.*, **12**(12), 1270-1280. https://doi.org/10.1177%2F073168449301201202.

Litak, G., J. Gajewski, A. Syta and J. Jonak (2008), "Quantitative estimation of the tool wear effects in a ripping head by recurrence plots", *J. Theoretical Appl. Mech.,* **46**(3), 521-530.

Madenci, E. (2019), "A refined functional and mixed formulation to static analyses of fgm beams", *Struct. Eng. Mech.,* **69**(4), 427-437. https://doi.org/10.12989/sem.2019.69.4.427.

Madenci, E., Y. O. Özkılıç and L. Gemi (2020), "Experimental and Theoretical Investigation on Flexure Performance of Pultruded GFRP Composite Beams with Damage Analyses", *Compos. Struct.*, 112162. https://doi.org/10.1016/j.compstruct.2020.112162.

Madenci, E. and A. Özütok (2020), "Variational approximate for high order bending analysis of laminated composite plates", *Struct. Eng. Mech.,* **73**(1), 97. https://doi.org/10.12989/sem.2020.73.1.097.

Mirjavadi, S. S., B. M. Afshari, N. Shafiei, A. Hamouda and M. Kazemi (2017), "Thermal vibration of two-dimensional functionally graded (2D-FG) porous Timoshenko nanobeams", *Steel Compos. Struct.,* **25**(4), 415-426. https://doi.org/10.12989/scs.2017.25.4.415.

Nejad, M. Z., A. Hadi and A. Farajpour (2017), "Consistent couple-stress theory for free vibration analysis of Euler-Bernoulli nano-beams made of arbitrary bi-directional functionally graded materials", *Struct. Eng. Mech.,* **63**(2), 161-169. https://doi.org/10.12989/sem.2017.63.2.161.

Nejad, M. Z., A. Hadi, A. Omidvari and A. Rastgoo (2018), "Bending analysis of bi-directional functionally graded Euler-Bernoulli nano-beams using integral form of Eringen's non-local elasticity theory", *Struct. Eng. Mech.,* **67**(4), 417-425. https://doi.org/10.12989/sem.2018.67.4.417.

Nguyen, T.-K., T. P. Vo and H.-T. Thai (2013), "Static and free vibration of axially loaded functionally graded beams based on the first-order shear deformation theory", *Compos. Part B. Eng.,* **55**, 147-157. https://doi.org/10.1016/j.compositesb.2013.06.011.

Nielsen, D. and R. Pitchumani (2001), "Intelligent model-based control of preform permeation in liquid composite molding processes, with online optimization", *Compos. Part A Appl. Sci. Manufact.,* **32**(12), 1789-1803. https://doi.org/10.1016/S1359-835X(01)00013-6.

Ozutok, A., E. Madenci and F. Kadioglu (2014), "Free vibration analysis of angle-ply laminate composite beams by mixed finite element formulation using the Gâteaux differential", *Sci. Eng. Compos. Mater.,* **21**(2), 257-266. https://doi.org/10.1515/secm-2013-0043.

Özütok, A. and E. Madenci (2013), "Free vibration analysis of cross-ply laminated composite beams by mixed finite element formulation", *J. Struct. Stabilibty Dynam.,* **13**(02), 1250056. https://doi.org/10.1142/S0219455412500563.

Özütok, A. and E. Madenci (2017), "Static analysis of laminated composite beams based on higher-order shear deformation theory by using mixed-type finite element method", *J. Mech. Sci.,* https://doi.org/10.1016/j.ijmecsci.2017.06.013.

Peng-hui, L., Z. Hong-ping, L. Hui and W. Shun (2015), "Structural damage identification based on genetically trained ANNs in beams", *Smart Struct. Syst.,* **15**(1), 227-244.

Pidaparti, R. and M. Palakal (1993), "Material model for composites using neural networks", *AIAA J.,* **31**(8), 1533-1535. https://doi.org/10.2514/3.11810.

Pradhan, K. and S. Chakraverty (2013), "Free vibration of Euler and Timoshenko functionally graded beams by Rayleigh–Ritz method", *Compos. Part B. Eng.,* **51**, 175-184. https://doi.org/10.1016/j.compositesb.2013.02.027.

Prakash, T. and M. Ganapathi (2006), "Asymmetric flexural vibration and thermoelastic stability of FGM circular plates using finite element method", *Compos. Part B. Eng.,* **37**(7-8), 642-649. https://doi.org/10.1016/j.compositesb.2006.03.005.

Rabia, B., T. H. Daouadji and R. Abderezak (2019), "Effect of porosity in interfacial stress analysis of perfect FGM beams reinforced with a porous functionally graded materials plate", *Struct. Eng. Mech.,* **72**(3), 293-304. https://doi.org/10.12989/sem.2019.72.3.293.

Raschka, S. (2015), *Python Machine Learning*, Packt Publishing Ltd., Birmingham, United Kingdom.

Rashid, T. (2016), *Make Your Own Neural Network*, CreateSpace Independent Publishing Platform, USA.

Rastbood, A., Y. Gholipour and A. Majdi (2017), "Stress Analysis of Segmental Tunnel Lining Using Artificial Neural Network", *Periodica Polytech. Civil Eng.,* **61**(4), 664-676. https://doi.org/10.3311/PPci.9700.

Sankar, B. (2001), "An elasticity solution for functionally graded beams", *Compos. Sci. Technol.,* **61**(5), 689-696. https://doi.org/10.1016/S0266-3538(01)00007-0.

Skorpil, V. and J. Stastny (2006), "Neural networks and back propagation algorithm", *Electron Bulg Sozopol*, 20-22.

Solmaz, S. and Ö. Civalek (2018), "Numerical Methods for FGM Composites Shells and Plates", *J. Eng. Appl. Sci.,* **10**(1), 5-12. http://dx.doi.org/10.24107/ijeas.415294.

Talha, M. and B. Singh (2010), "Static response and free vibration analysis of FGM plates using higher order shear deformation theory", *Appl. Math. Modell.,***34**(12), 3991-4011. https://doi.org/10.1016/j.apm.2010.03.034.

Trinh1a, T.-H., D.-K. Nguyen2b, B. S. Gan and S. Alexandrov3c (2016), "Post-buckling responses of elastoplastic FGM beams on nonlinear elastic foundation", *Struct. Eng. Mech.,* **58**(3), 515-532. http://dx.doi.org/10.12989/sem.2016.58.3.515.

Twomey, J. and A. Smith (1995), "Performance measures, consistency, and power for artificial neural network models", *Math. Comput. Modell.,***21**(1-2), 243-258. https://doi.org/10.1016/0895-7177(94)00207-5.

Wang, B., J. H. Ma and Y. P. Wu (2013), "Application of artificial neural network in prediction of abrasion of rubber composites", *Mater. Design*, **49**, 802-807. https://doi.org/10.1016/j.matdes.2013.01.047.

Yadav, A. K., H. Malik and A. Mittal (2015), "Artificial neural network fitting tool based prediction of solar radiation for identifying solar power potential"*, J. Electr. Eng,* **15**(2), 25-29.

Yavuz, G. (2016), "Shear strength estimation of RC deep beams using the ANN and strut-and-tie approaches", *Struct. Eng. Mech.,* **57**(4), 657-680. https://doi.org/10.12989/sem.2016.57.4.657.

Zhang, D.-G. and Y.-H. Zhou (2008), "A theoretical analysis of FGM thin plates based on physical neutral surface", *Comput. Mater. Sci.,* **44**(2), 716-720. A theoretical analysis of FGM thin plates based on physical neutral surface.

Zhang, Z. and K. Friedrich (2003), "Artificial neural networks applied to polymer composites: A review", *Compos. Sci. Technol.,* **63**(14), 2029-2044. https://doi.org/10.1016/S0266-3538(03)00106-4.

Zhao, Y., M. Noori and W. A. Altabey (2017), "Damage detection for a beam under transient excitation via three different algorithms", *Struct. Eng. Mech.,* **64**(6), 803-817. https://doi.org/10.12989/sem.2017.64.6.803.

Ziane, N., S. A. Meftah, G. Ruta, A. Tounsi and E. A. Adda Bedia (2015), "Investigation of the Instability of FGM box beams", *Struct. Eng. Mech.,* **54**(3), 579-595. https://doi.org/10.12989/sem.2015.54.3.579.

Zine, A., A. Tounsi, K. Draiche, M. Sekkal and S. Mahmoud (2018), "A novel higher-order shear deformation theory for bending and free vibration analysis of isotropic and multilayered plates and shells", *Steel Compos. Struct.,* **26**(2), 125-137. https://doi.org/10.1016/j.compstruct.2012.08.025.

*CC*